Coefficient of restitution as a fluctuating quantity

Marina Montaine,[1] Michael Heckel,[1] Christof Kruelle,[2] Thomas Schwager,[3] and Thorsten Pöschel[1]
[1]*Institute for Multiscale Simulation, Friedrich-Alexander Universität Erlangen-Nürnberg, Erlangen, Germany*
[2]*Hochschule Karlsruhe, Fakultät für Maschinenbau und Mechatronik, Karlsruhe, Germany*
[3]*Bruker Nano GmbH, Berlin, Germany*

(Received 1 April 2011; revised manuscript received 23 August 2011; published 21 October 2011)

The coefficient of restitution of a spherical particle in contact with a flat plate is investigated as a function of the impact velocity. As an experimental observation we notice nontrivial (non-Gaussian) fluctuations of the measured values. For a fixed impact velocity, the probability density of the coefficient of restitution, $p(\varepsilon)$, is formed by two exponential functions (one increasing, one decreasing) of different slope. This behavior may be explained by a certain roughness of the particle which leads to energy transfer between the linear and rotational degrees of freedom.

DOI: 10.1103/PhysRevE.84.041306 PACS number(s): 45.70.−n, 45.50.Tn, 45.05.+x

I. INTRODUCTION

The dissipative collision of a solid particle with a hard plane may be described by the coefficient of normal restitution,

$$\varepsilon = -\frac{\boldsymbol{v}' \cdot \boldsymbol{n}}{\boldsymbol{v} \cdot \boldsymbol{n}}, \tag{1}$$

relating the normal components of the relative velocity before and after a collision at the point of contact. The unit vector $\boldsymbol{n}$ indicates the direction normal to the plane. Obviously, $\varepsilon = 1$ stands for elastic collisions whereas $\varepsilon = 0$ indicates the complete dissipation of the energy of the relative motion. There are several techniques for measuring the coefficient of restitution, including high-speed video analysis (see, e.g., [1]) and sophisticated techniques where the particle is attached to a compound pendulum with the axis of rotation very close to the center of mass [2,3], which makes this method particularly suitable for the measurement of the coefficient of restitution for very small impact velocities down to mm/s and below. In the presence of gravity, the coefficient of restitution can be measured by determining the time lag between consecutive impacts of a particle bouncing on a hard plane by using a piezoelectric force sensor (see, e.g., [4,5]) or an accelerometer mounted to the plate, which detects elastic waves excited by the impact (see, e.g., [6]). When both particle and plate are metallic, the time of the impacts can be determined by applying a dc voltage between ball and plate and determining the instant when the circuit closes [6]. In many papers, the time lag and, thus, ε is determined by recording the sound emitted from a spherical particle bouncing on an underlying flat plane (see, e.g., [7,8] and many others). From the times t_i of impacts one can compute the coefficient of restitution via

$$\varepsilon(v_i) = \frac{v_i'}{v_i} = \frac{t_{i+1} - t_i}{t_i - t_{i-1}}, \quad v_i = \frac{g}{2}(t_i - t_{i-1}), \tag{2}$$

where v_i and v_i' are the normal pre- and postcollisional velocities of the impact taking place at time t_i and g is the acceleration due to gravity.

Although it is frequently assumed that the coefficient of restitution is a material constant (e.g., this assumption is common in many textbooks and widely used in simulations), numerous experimental studies have revealed that it depends on many parameters: impact velocity, material characteristics of the impacted bodies, particle size, shape, roughness, and surface properties like adhesion. Here we restrict ourselves to the investigation of ε of a single dry steel ball bouncing on a hard plane such that the coefficient of restitution is only a function of the impact velocity $\varepsilon = \varepsilon(v)$ and the surface properties characterized by microscopic asperities.

If the particle was a perfect sphere and the plane was perfectly flat, the coefficient of restitution would be a deterministic function of the system parameters. In this case, fluctuations of the measured values would be caused exclusively by imperfections of the experiment. However, in several experimental investigations, using either photographic techniques [9] or an acoustic emission analysis [5,6], an extraordinary high fluctuation level was noticed whose origin remained obscure and cannot be attributed to the imperfections of the measurements (see below). In this paper, by means of large-scale experiments as well as micromechanical modeling we make an attempt to characterize the fluctuations of the coefficient of restitution and to explain the mechanism leading to these fluctuations.

II. EXPERIMENTS

For the experiments we use a robot to move a small vertical tube to a desired position $\{x,y,z\}$. In the beginning of each experimental trial a stainless steel bearing ball is suspended at the end of the tube by means of a vacuum pump. Upon switching off the pump, the sphere is released to bounce repeatedly off the ground where the sound is recorded by a piezoelectric sensor. When the ball eventually comes to rest, it is pushed to a defined position by a fan where it is picked up by the robot who moves the ball again to the start position for the next trial. In each cycle the initial $\{x,y\}$ position is chosen randomly within the central region of the ground plate such that edge effects [10] are not noticeable. The dropping height is chosen randomly from $z \in [9,10]$ cm, corresponding to initial impact velocities $v \in [1.33,1.4]$ m/s, which allows for the observation of 90 to 100 bounces of the ball. A massive hard glass plate of size $30 \times 20 \times 1.9$ cm^3 serves as a ground plate for the experiment. The measuring process is fully automatized, which allows us to perform a large-scale experiment collecting data from thousands of bouncing-ball

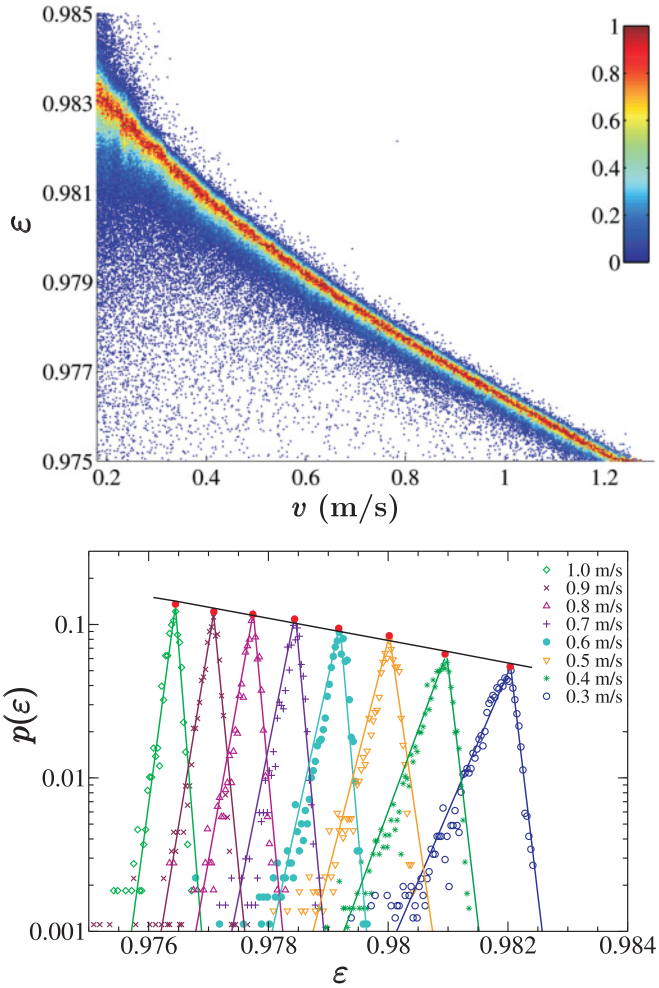

FIG. 1. (Color online) Experimental results. Top: Coefficient of restitution ε plotted against the normal impact velocity v. The data (200 000 data points) are colored according to the normalized frequency of occurrences. Bottom: Histograms of ε for impact velocities from small intervals, centered around $v = 0.3, \ldots, 1.0$ m/s. The lines are exponential fits.

trials. To assure stationary conditions, the temperature and humidity of the experimental environment were kept constant.

From the analysis of the sound-sensor signal we obtain the impact times t_i and, thus, via Eq. (2) the normal impact velocities v_i and the coefficients of restitution $\varepsilon(v_i)$. Figure 1 displays the abundance of data, $\varepsilon(v)$, for a stainless steel ball (radius $R = 3.0$ mm, Young's modulus $Y = 200$ GPa, Poisson ratio $\nu = 0.30$, density $\rho_s = 7.90$ g/cm^3). Besides the expected decay of ε with increasing impact velocity (see, e.g., [11,12]), we observe a large scatter of the data. The scatter of the data increases appreciably with decreasing impact velocity. An analogous trend can also be noticed from the data presented in [6], but was not found in earlier similar experiments [4,5]. We wish to note that the experiment in [6] corresponds to a completely different regime. There, the impact velocity where the fluctuations adopt their largest values corresponds to a jumping height of only 51 nm; therefore, we believe that the fluctuations in [6] and the fluctuations reported here are of different origin.

The fluctuations seem to be small; however, if only the uncertainty (here $\Delta t = 2\ \mu$s) of the measurement of t_i was responsible for the scatter, one would expect fluctuations of the measured coefficient of restitution in the range of 0.024% for the last impacts ($v \approx 0.2$ m/s) while we observe fluctuations of the order of 1%.

The scatter of ε is asymmetric; that is, the deviation of the data with ε lower than the mean is noticeably larger. This can be seen also in Fig. 1 (bottom), which shows the normalized frequency $p(\varepsilon)$ of measurements of a certain value of ε for several small intervals of the impact velocity v. Thus, if we consider ε as a fluctuating quantity, $p(\varepsilon)$ is its probability density function. This function reveals strongly non-Gaussian behavior, but the distribution is shaped by a combination of two exponential functions (one increasing, one decreasing) of different slope. By detailed error analysis, we can exclude that these uncommon statistical properties are due to imperfections of the measurements but are a consequence of microscopic asperities at the sphere's surface. This hypothesis is checked below by means of a numerical simulation.

Note that the data presented in Fig. 1 are not an universal description of the fluctuations as a function of impact velocity. Since the sphere was released from approximately the same height, the data for different velocities, $v \approx (1.2, \ldots, 0.2)$ m/s correspond to different impact numbers, $N \approx (3, \ldots, 90)$. Alternatively, one could plot the function $p(\varepsilon)$ separately for fixed impact number by varying the initial height. While in simulations (see next section) we could generate the plot $p(\varepsilon)$ separately for fixed number of impacts; in the experiment we cannot since this would require us to vary the initial height over a very large interval (millimeters to kilometers) which is neither experimentally feasible nor in agreement with the assumption that plastic deformations and air drag are negligible.

The stationarity of the experiment deserves some discussion: The experiment is repeated many thousands of times using the same sphere; thus, the sphere has undergone a total of about 2×10^6 collisions. The mechanical setup of the experiment would be significantly simpler if we would use not a single sphere but many virtually identical spheres. However, since we are looking for small fluctuations of the coefficient of restitution we had to exclude that these fluctuations originate from the statistical scatter of the surface and bulk properties of different spheres. For stationarity, we have to assure that the surfaces of the plane and the sphere remain invariant. We analyzed the surface of the sphere by means of a Scanning Electron Microscope (SEM) close to the beginning of the experiment (after about 100 000 bounces which were not used for the statistics) and close to the end of the experiment. As a result, no significant differences could be seen, neither regarding the circularity of the ball nor the surface properties. While the surface reveals some tiny scratches, the structure of the surface remains approximately invariant. During the experiment a small part of the plate was covered from impacts to serve as a reference for damage analysis. Regular visual inspection did not show any damage of the plate. As an *à posteriori* argument, we analyzed the statistics of the fluctuations using only data from the first 10% of the impacts and from the last 10% separately. Both sets of data lead to identical statistics up to fluctuations; thus, no significant influence of wear was apparent.

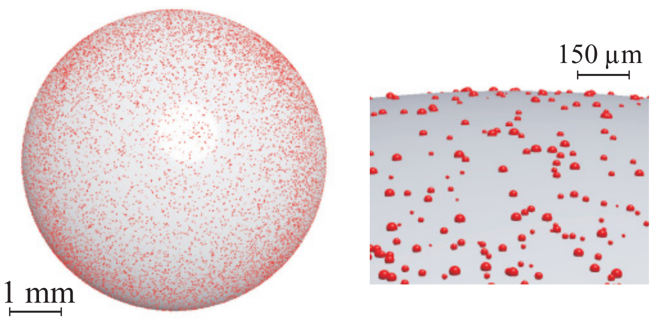

FIG. 2. (Color online) Sketch of the particle model and closeup of its surface.

III. NUMERICAL SIMULATIONS

The procedure of our simulation is analogous to the experiment; the rigid ball is dropped from a certain height h and repeatedly collides with a smooth, hard plate. Air drag is neglected[1] and the ball is subjected only to gravity.

The ball is modeled as a composite multisphere particle (Fig. 2).

The large central sphere of radius R is randomly covered by many tiny spheres of different microscopic size, representing asperities due to surface roughness. The center of each small sphere i of radius R_i is located at the surface of the central sphere. The number of asperities $N \sim 10^6$ and their maximal size $R_i/R \sim 10^{-3}$ corresponds to a coverage of about 25%, which is in approximate agreement with the coverage of the surface by small scratches seen in SEM pictures. Since the mass ratio $m_i/m \sim 10^{-9}$ we can safely neglect the contribution of the small particles for the computation of the moment of inertia of the ball. Thus, the ball is characterized by its mass m, R, center-of-mass velocity $\boldsymbol{v}_G$, angular velocity $\boldsymbol{\omega}$, the set of the radii, R_i, of the asperities, and the set of their position vectors, $\boldsymbol{r}_i$, pointing from the center of the large sphere to the asperities. Note that there is an important difference between the surface texture of the sphere (the experiment) and the asperities intended to represent roughness in the model: The scratches and other imperfections of the sphere originate from microscopical plastic deformations while the asperities of the model are invariant. Thus, the texture of the sphere changes permanently due to impacts. However, since after some relaxation the surface texture is statistically invariant as seen from SEM images and by comparing the first 10% of the data with the last 10%, the model with invariant asperities seems to be appropriate.

When bouncing, the ball may come in contact with the plane either through the central sphere or through one of the asperities. In both cases the collision is assumed instantaneous and inelastic, characterized by coefficients of restitution. In the intervals between collisions the ball follows a ballistic trajectory,

$$\boldsymbol{r}_G(t) = \boldsymbol{r}_G(t_0) + \boldsymbol{v}_G(t_0)(t - t_0) + \frac{(t-t_0)^2}{2}\boldsymbol{g}, \quad t \geqslant t_0, \quad (3)$$

where t_0 is the time of the preceding collision and $\boldsymbol{g}$ is gravity while the angular velocity $\boldsymbol{\omega} \equiv \omega \boldsymbol{e}_\omega$ remains constant. The evolution of a vector $\boldsymbol{p}$ fixed to the particle is then given by

$$\begin{aligned}\boldsymbol{p}_{rot} &= \boldsymbol{p}\cos\omega t + \boldsymbol{e}_\omega(\boldsymbol{e}_\omega\cdot\boldsymbol{p})(1-\cos\omega t) + (\boldsymbol{e}_\omega \times \boldsymbol{p})\sin\omega t \\ &= \hat{A}(t)\boldsymbol{p}, \end{aligned} \quad (4)$$

which defines the rotation matrix $\hat{A}$ [13]. Therefore, the particle contacts the ground when the center of the first asperity j reaches the height R_j; that is, the time t_c of contact follows from the condition

$$\min_{j=1,N}[\boldsymbol{r}_G(t_c) + \hat{A}(t_c)\boldsymbol{r}_j]_z = R_j, \quad (5)$$

where $[\cdots]_z$ means the vertical component of the argument. The vectorial impact velocity at the point of contact $\boldsymbol{r}_c$ is then

$$\boldsymbol{v}_c = (\boldsymbol{v}_c\cdot\boldsymbol{n})\boldsymbol{n} + (\boldsymbol{v}_c\cdot\boldsymbol{t})\boldsymbol{t} = \boldsymbol{v}_G + \boldsymbol{\omega}\times\boldsymbol{r}_c, \quad (6)$$

where $\boldsymbol{n}$ and $\boldsymbol{t}$ are the unit vectors in normal and tangential directions (see Fig. 3).

The postcollisional velocity at the contact point is given by

$$\boldsymbol{v}_c'\cdot\boldsymbol{n} = -\varepsilon\,(\boldsymbol{v}_c\cdot\boldsymbol{n}), \quad \boldsymbol{v}_c'\cdot\boldsymbol{t} = \beta\,(\boldsymbol{v}_c\cdot\boldsymbol{t}), \quad (7)$$

with the coefficients of normal and tangential restitution ε and β. Finally, we compute the postcollisional velocity $\boldsymbol{v}_G'$ and angular velocity $\boldsymbol{\omega}'$:

$$\begin{aligned}\boldsymbol{v}_G' - \boldsymbol{v}_G &= \Delta\boldsymbol{v}_G = \frac{1}{m}\boldsymbol{P}, \\ \boldsymbol{\omega}' - \boldsymbol{\omega} &= \Delta\boldsymbol{\omega} = \frac{1}{\hat{J}}\boldsymbol{r}_c\times\boldsymbol{P},\end{aligned} \quad (8)$$

where the transferred momentum $\boldsymbol{P}$ is obtained from Eqs. (6) and (7):

$$\boldsymbol{v}_c' - \boldsymbol{v}_c = \Delta\boldsymbol{v}_G + \Delta\boldsymbol{\omega}\times\boldsymbol{r}_c = \frac{1}{m}\boldsymbol{P} + \frac{1}{\hat{J}}(\boldsymbol{r}_c\times\boldsymbol{P})\times\boldsymbol{r}_c, \quad (9)$$

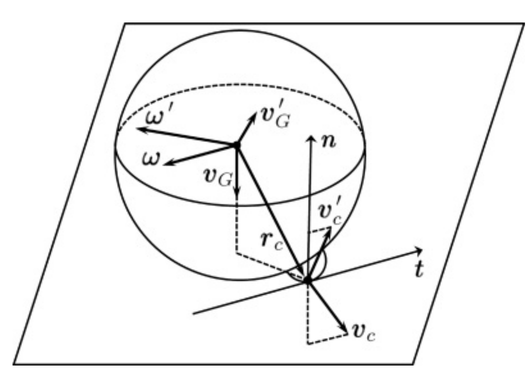

FIG. 3. Sketch of a particle collision. For simplicity, only the impacting asperity (of exaggerated size) is drawn.

[1]For the measured range of impact velocities and given particle size and mass the neglect of air resistance causes a minor systematic error since both intervals $t_{i+1} - t_i$ and $t_i - t_{i-1}$ [see Eq. (2)] are shorter due to air drag. Assuming the air drag force is proportional to the square of the velocity of the particle, we obtain the relative error $\|\varepsilon^{\text{air}} - \varepsilon\|/\varepsilon \approx 1.8 \times 10^{-5}$ to 9.4×10^{-4} for the measured ranges of impact velocity $v \in [0.1, 1.4]$ m/s and coefficient of restitution $\varepsilon \in [0.974, 0.985]$. This deviation is far below the resolution of our data; thus, the influence of air drag can be safely neglected. Moreover, the influence of air drag is a systematic effect that does not concern the fluctuations of the coefficient of restitution in which we are interested.

with the mass m and the moment of inertia $\hat{J}$ of the particle.

Using Eqs. (5) and (8) we can compute the dynamics of the bouncing particle and, in particular, the times and velocities of the impacts, while the coefficients of restitution ε and β are given. For ε as a function of the normal impact velocity v_c we use the expression for viscoelastic spheres [12]

$$\varepsilon(v_c) = 1 + \sum_{i=1}^{\infty} C_i A_i (v_c)^{i/10}, \tag{10}$$

with C_i being known constants ($C_1 = C_3 = 0$, $C_2 = -1.153$, $C_4 = 0.798$, $C_5 = 0.267, \ldots,$ see [12] for details) and A_i being material constants. We determined the first three nontrivial constants, $A_2 \approx 0.0467$, $A_4 \approx 0.1339$, and $A_5 \approx -0.2876$ by fitting Eq. (10) to the experimental data shown in Fig. 1.

The coefficient β of tangential restitution depends on both bulk material properties and surface properties. Therefore, β cannot be analytically derived from material properties, except for the limiting case of pure Coulomb friction [14]. Here, we use $\beta = 1$.

IV. SIMULATION RESULTS

On the macroscopic level (neglecting the microscopic asperities at the surface of the particle), the simulation results can be analyzed in the same way as the experimental data. We introduce the macroscopic coefficient of restitution $\tilde{\varepsilon}$ as the ratio of the postcollisional to precollisional center-of-mass velocities in the normal direction:

$$\tilde{\varepsilon} = -\frac{\boldsymbol{v}'_G \cdot \boldsymbol{n}}{\boldsymbol{v}_G \cdot \boldsymbol{n}}. \tag{11}$$

Surprisingly, the macroscopic interpretation of our simulation results depicted in Fig. 4 shows a striking resemblance to the experimental data. While the actual coefficient of normal restitution ε is a function of the normal impact velocity described by Eq. (10), the macroscopic coefficient of restitution $\tilde{\varepsilon}$ computed via Eq. (11) reveals strong fluctuations, in agreement with the experiment.

The probability densities $p(\tilde{\varepsilon})$ (bottom panel of Fig. 4) are also close to the distribution obtained in the experiment. Their shape is excellently approximated by a combination of two exponential functions, one increasing and one decreasing. The peaks of $p(\tilde{\varepsilon})$ are in line with the values of $\varepsilon(v_G)$ obtained from Eq. (10) for the corresponding velocities.

For the case of an absolutely smooth particle (no asperities), the impact velocity $\boldsymbol{v}_c$ at the point of contact is the same as $\boldsymbol{v}_G$ and $\tilde{\varepsilon}$ is equal to the coefficient of normal restitution ε. Therefore, in this case, there would be no scatter of the measured values of $\tilde{\varepsilon}$. Consequently, the scatter in these data must be attributed to the asperities at the surface of the particle. From the agreement of the experimental data (Fig. 1) and the simulation data (Fig. 4), it became apparent that the tiny microscopic imperfections of the surface of the otherwise macroscopically smooth particle lead to the characteristic fluctuations of the coefficient of normal restitution. One notices a slight asymmetry in the shape of the probability density in case of the experimental results [i.e., $p(\varepsilon)$ compared to $p(\tilde{\varepsilon})$]. We believe that this asymmetry may be attributed to additional dissipative forces that were not taken into account in our model.

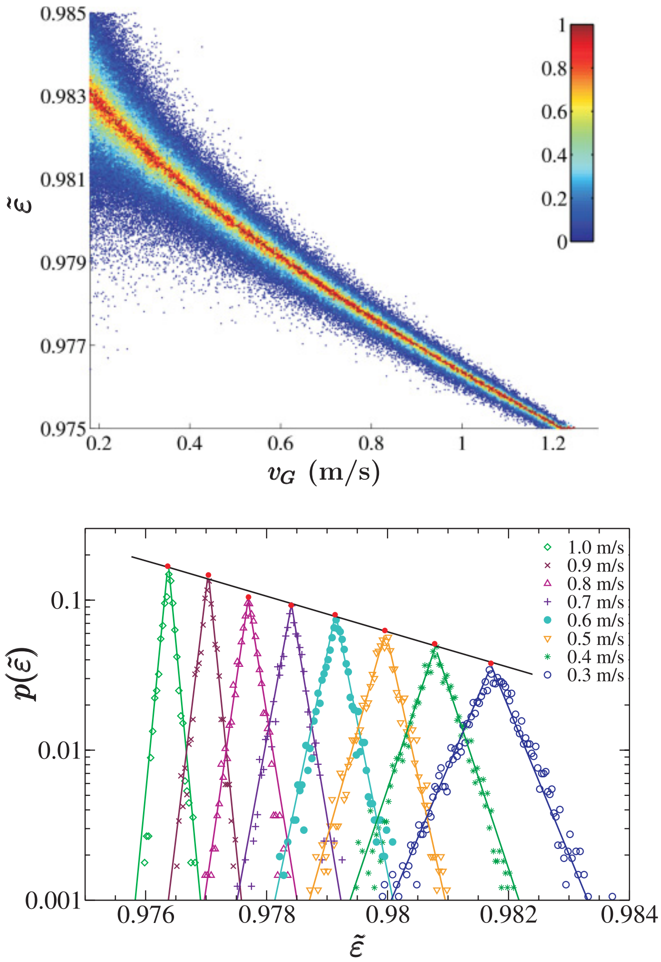

FIG. 4. (Color online) Simulation results. Top: The macroscopic coefficient of restitution $\tilde{\varepsilon}$ plotted against the normal center-of-mass velocity v_G at the moment of impact. The data (200 000 data points) are colored according to the normalized frequency of occurrences. Bottom: Histograms of $\tilde{\varepsilon}$ for velocities from small intervals, centered around $v_G = 0.3, \ldots, 1.0$ m/s. The lines are exponential fits.

Let us consider the role of the sphere's rotational degrees of freedom, which may be interpreted as internal degrees of freedom since they do not enter the computation of the coefficient of restitution, neither in the experiment Eq. (2) nor in the simulation Eq. (11). Initially, the particle had no spin and only one degree of freedom in its translational motion. However, due to eccentric impacts caused by asperities, the particle gains some rotation and acquires velocity in the horizontal direction. The partition of total kinetic energy in rotational and translational degrees of freedom constantly varies from one impact to another. Thus, the kinetic energy of the linear vertical motion (the only component which enters ε) just before a collision is transformed into energy of the rebound vertical velocity, dissipated energy due to the coefficient of restitution, and changes in the horizontal and rotational velocities. The latter two contribution may be positive or negative, leading to a reduced or increased value of the measured coefficient of restitution, according to Eqs. (2) and (11). Therefore, the particle rotation may be considered as a reservoir of internal energy, leading to fluctuations of the measured coefficient of restitution.

The substantial increase of scatter in the data with the decrease of impact velocity can be attributed to the growing role of the rotational degrees of freedom in the energy partition. In consecutive collisions the translational energy decreases appreciably due to dissipation, but the amount of energy concentrated in rotation varies only slightly. Thus, the proportion of rotational to translational energy increases with the number of particle bounces. The kinetic energy transfers from the rotational to translational mode and vice versa result in a more apparent fluctuation of the coefficient of restitution. As a consequence, the scattering of the restitution coefficient increases as the impact velocity decreases.

V. CONCLUSION

We have performed an experimental and numerical study of the coefficient of normal restitution as a function of impact velocity. From about 2.2×10^6 experiments of the same stainless steel sphere bouncing on a massive horizontal plate, we determined experimentally the probability distribution of the fluctuations of the coefficient of normal restitution, ε. We found that ε increases as the impact velocity decreases. For fixed impact velocity, the probability density of the coefficient of restitution, $p(\varepsilon)$, is non-Gaussian. It consists of two exponential functions (one increasing, one decreasing) of different slope. We modeled the particle used in the experiment by a mathematical sphere whose surface is covered by a large number of much smaller spheres (asperities) to simulate a certain roughness. The simulations revealed the same properties of the fluctuations. Since the asperities are the only origin of scatter in our simulation model, we conclude that the experimentally observed fluctuations of the coefficient of restitution coefficient are due to microscopic surface roughness of the ball, causing energy transfer between the translational and rotational degrees of freedom.

ACKNOWLEDGMENTS

We thank Knut Reinhardt for technical assistance in setting up the robot, Benjamin Butz and Erdmann Spiecker for SEM microscopy, and Deutsche Forschungsgemeinschaft (DFG) for funding through the Cluster of Excellence Engineering of Advanced Materials.

[1] L. Labous, A. D. Rosato, and R. N. Dave, Phys. Rev. E **56**, 5717 (1997).
[2] F. G. Bridges, A. Hatzes, and D. N. C. Lin, Nature (London) **309**, 333 (1984).
[3] A. Hatzes, F. G. Bridges, and D. N. C. Lin, Mon. Not. R. Astron. Soc. **231**, 1091 (1988).
[4] M. G. Koller and H. Kolsky, Int. J. Solids Struct. **23**, 1387 (1987).
[5] E. Falcon, C. Laroche, S. Fauve, and C. Coste, Eur. Phys. J. B **3**, 45 (1998).
[6] H. King, R. White, I. Maxwell, and N. Menon, Europhys. Lett. **93**, 14002 (2011).
[7] A. D. Bernstein, Am. J. Phys. **45**, 41 (1977).
[8] I. Stensgaard and E. Lægsgaard, Am. J. Phys. **69**, 301 (2001).
[9] C. M. Sorace, M. Y. Louge, M. D. Crozier, and V. H. C. Law, Mech. Res. Comm. **36**, 364 (2009).
[10] R. Sondergaard, K. Chaney, and C. E. Brennen, J. Appl. Mech. **57**, 694 (1990).
[11] N. V. Brilliantov, F. Spahn, J.-M. Hertzsch, and T. Pöschel, Physica A **231**, 417 (1996).
[12] T. Schwager and T. Pöschel, Phys. Rev. E **78**, 051304 (2008).
[13] H. Goldstein, C. P. Poole, and J. L. Safko, *Classical Mechanics* (Addison Wesley, San Francisco, 2001).
[14] T. Schwager, V. Becker, and T. Pöschel, Eur. Phys. J. E **27**, 107 (2008).